JOURNAL OF GEOPHYSICAL RESEARCH, VOL. 101, NO. B12, PAGES 28,165–28,175, DECEMBER 10, 1996

Scale-invariant topography and porosity variations in fluvial sedimentary basins

J. D. Pelletier and D. L. Turcotte

Department of Geological Sciences, Cornell University, Ithaca, New York

Abstract. We consider a model of a floodplain evolving with channel avulsion, deposition, and erosion. Avulsion is modeled as a random process in space and time. Sediment transport is modeled by the diffusion equation (Culling's model). The power spectrum of variations in the topographic profiles predicted by the model $S(k)$ is proportional to k^{-2} (where k is the wavenumber). This is the Brown noise often observed in topography. The power spectrum of variations in the local elevation in time is proportional to $f^{-3/2}$ (where f is the frequency). The model prediction of Brown noise floodplain topography is roughly consistent with spectral analyses of microtopography measured with laser altimetry. We inferred Brown noise paleotopography by comparing the pair correlation function of showing wells in the Denver and Powder River basins with a synthetic oil field based on a caprock with Brown noise topography. Topographic control of variations in the grain size of deposited sediment suggests that porosity variations may exhibit the scale invariance predicted for the topographic profile. To illustrate vertical scale invariance in porosity variations, we computed the power spectrum of vertical porosity well logs in 15 offshore wells in the Gulf of Mexico. At spatial scales above 3 m we find an average power spectral exponent of −1.4, close to our model prediction of −1.5.

Introduction

In a landmark paper, *Hewett* [1986] presented a time series analysis of a vertical porosity well log from a submarine fan. He showed that variations in this log were scale invariant over a wide range of scales. Scale-invariance means that the power spectrum follows a power law dependence on wavenumber k: $S(k) \propto k^{-\beta}$. Similar scale invariant power spectra for a variety of well log types were reported by *Walden and Hosken* [1985], *Pilkington and Todoeschuck* [1990], *Todoeschuck et al.* [1990], and *Holliger* [1996]. *Todoeschuck and Jensen* [1989] explored the implications of scale invariant variations to seismic deconvolution. *Tubman and Crane* [1995] showed scale invariant spectra for horizontal well logs in fluvial sedimentary environments. Based on his original observation, Hewett developed a fractal-based interpolation scheme for determining the three-dimensional porosity variations in sedimentary basins using logs from wells scattered in the basin. He was able to construct realistic and accurate sedimentary structures. This approach was applied to groundwater migration by *Molz and Boman* [1993]. H. A. Makse et al. [Quantitative characterization of permeability fluctuations in sandstone, unpublished manuscript, 1995] have recently analyzed porosity variations at the millimeter scale with the rescaled-range analysis. They obtained results very similar to those of *Hewett* [1986] who applied the rescaled-range analysis to variations on much larger scales.

It is the purpose of this paper to present a model for the topography and porosity variations in fluvial sedimentary basins that produces the observed scale invariant behavior on the scale of meters to tens of kilometers. Fluvial sedimentary basins exhibit heterogeneity on all of these scales. Heterogeneity at the largest scale is associated with the boundaries of major genetic units of sediment such as channel belts. From scales of centimeters to tens of meters, heterogeneities are associated with variations in porosity within the larger genetic units such as coarse-fine stratification of a point bar [*Allen and Allen*, 1990]. The genetic units are usually positioned relative to each other in a complex, often interconnected geometry. A major problem in formation evaluation is determining the interconnectedness of the units [*Hirst et al.*, 1993].

Models of fluvial reservoir heterogeneity by allocyclic processes (those generated within the basin) focus on channel avulsion, a channel's abandonment of its belt in favor of a new course (resulting in first-order heterogeneity) and sediment transport (spatial variations of which result in second-order heterogeneity). In previous modeling efforts, channel avulsion, due to its complexity and unpredictability, has often been modeled as

Paper number 96JB02848.
0148-0227/96/96JB0284809.00

a stochastic process. The time between avulsions has been chosen from a uniform [*Leeder*, 1978] or a Weibull distribution [*Bridge and Leeder*, 1979]. The new channel belt was either positioned randomly on the floodplain [*Leeder*, 1978] or was placed at the lowest point of a section [*Bridge and Leeder*, 1979]. *Mackey and Bridge* [1995] chose a probability of avulsion dependent on the local gradient of the surface. An important aspect of their simulation results is the control of the new location of channel belts by the topographic profile of the floodplain perpendicular to the flow direction. They found that channel belts may be clustered preferentially on one side of the floodplain if a large alluvial ridge is present [*Mackey and Bridge*, 1995]. This clustering is directly analagous to the clustering of porosity variations inplied by power law power spectra.

In a laboratory study, *Hooke and Rohrer* [1979] have computed transition matrices to describe the probability of avulsion from a channel of one height along the topographic profile perpendicular to the channel direction to another height on laboratory alluvial fans. They observed that avulsion probabilities were significantly affected by the previous history of avulsion and deposition as represented by the topographic profile. For instance, they identified sequences in which areas of the fan which flow had not reached for some time would experience abrupt and lengthy deposition once aggradation ensued. They also found that the topographic profile had a nearly Gaussian distribution of values about the mean for both laboratory and natural alluvial fans, suggesting that a stochastic model is appropriate.

The dominant feature resulting from sediment transport on a floodplain is the gradual decrease in thickness and grain size of deposited sediment away from channels in the direction perpendicular to the channel [J. S. Bridge, Fluvial Sedimentology: A short course, unpublished manuscript, 1995, hereinafter referred to as J. S. Bridge, unpublished manuscript, 1995]. Although the mechanics of sediment transport are complex, a simple diffusion model has been successfully applied to the profile of sediment thickness and grain size perpendicular to the channel direction [*Pizzuto*, 1987]. The diffusion equation is perhaps the most widely used model in hillslope evolution. *Culling* [1965] hypothesized that the horizontal flux of eroded material was proportional to the slope. With conservation of mass this yields the diffusion equation [*Turcotte*, 1992]. Solutions to the diffusion equation have been applied successfully to model alluvial fans, prograding deltas, and eroding fault scarps [*Wallace*, 1977; *Nash*, 1980a, b; *Hanks et al.*, 1984; *Hanks and Wallace*, 1985; *Kenyon and Turcotte*, 1985].

In this paper we present a model for the development of a fluvial sedimentary basin by channel avulsion modeled as a random process and deposition governed by the diffusion equation. Our model describes the evolution of the topographic profile perpendicular to the large-scale slope of the alluvial plain. We also model the effects of erosion. Our results are independent of the different parameterizations of erosion. Many previous simulations of alluvial stratigraphic architecture have included the effects of autocyclic processes such as tectonic and climatic forcing. We do not include these effects in our model. We consider both a continuous and a discrete model and discuss their solutions in detail. We begin by idealizing the channels as parallel and uniform in capacity along the downslope direction. This reduces the model to two spatial dimensions: the height of the topographic profile (denoted h) the strike direction (denoted x). The equation describing the continuous version of the model is known as the Edwards-Wilkinson model in the physics literature on stochastic surface growth [*Edwards and Wilkinson*, 1982]. The power spectrum of the topographic profile perpendicular to the channel direction predicted by the model $S(k)$ is proportional to k^{-2} (where k is the wavenumber). This is the Brown noise often observed in topography [*Fox and Hayes*, 1985]. The power spectrum of variations in local elevation in time is proportional to $f^{-3/2}$ (where f is the frequency). We show that these power spectra are unchanged when we relax the condition of parallel channels to include any angular probability distribution of channel directions, extending the model to three dimensions. *Dunne et al.* [1995] have performed spectral analysis of transects of fluvial microtopography perpendicular to the hillslope fall line. They obtained power spectra roughly consistent with the model prediction of $S(k) \propto k^{-2}$. In addition, we inferred Brown noise paleotopography by comparing the pair correlation function of showing wells in the Denver and Powder River basins with a synthetic oil field based on a caprock with Brownian topography. We argue that Brown noise topography is also consistent with the fractal dimensions of the perimeters of sand isopachs measured by *Agterberg* [1982] and the size distribution of oil fields given by *Barton and Scholz* [1995]. In a similar application of stochastic surface growth models to the fractal geometry often observed in the Earth sciences, *Sornette and Zhang* [1993] applied the Kardar-Parisi-Zhang model, a nonlinear extension of the Edwards-Wilkinson model, to the fractal structure of erosional topography in general. A fundamental question in geophysics is why the topographic profiles of the Earth, Mars, and Venus all resemble a Brownian walk despite the variety of tectonic and geomorphological processes which operate on those planets [*Turcotte*, 1987]. We do not attempt to answer that question. We attempt only to present a model for scale invariant topography in a fluvial sedimentary basin, where channel belts have a simpler geometry than that of a highly branched river network.

Grain size variations are coupled to the topographic profile perpendicular to the channel direction with the coarsest material deposited at the channel banks and finer sediment deposited in topographic depressions such as abandoned channel segments [J. S. Bridge, unpublished manuscript, 1995]. This suggests the possibility that porosity variations may exhibit the same power spectral dependence as the topographic profile. To illustrate vertical scale invariance in porosity variations, we computed the power spectrum of vertical porosity well logs in 15 offshore wells in the Gulf of Mexico. At spatial scales above 3 m we find an average power spectral exponent of −1.4, close to our model prediction of −1.5.

The logical structure and major points of our paper can be summarized:

1. Diffusive sediment transport with random erosion and deposition along channels produces fractal topographic variations in space ($S(k) \propto k^{-2}$) and time ($S(f) \propto f^{-3/2}$).

2. Porosity variations mimic topographic variations. As such, porosity variations with depth mimic variations of the local topography in time.

3. Observations show that porosity variations vertically in sedimentary basins are scale invariant with similar power spectral exponents as that predicted for the variation of the local topography in time.

4. Power spectral analyses of fluvial microtopography yield spectra close to that of Brown noise ($S(k) \propto k^{-2}$).

5. Hydrocarbons migrate upward until the crests of low-porosity caprock obstruct progress. The observed spatial clustering of hydrocarbons is consistent with those of a synthetic oil field with a Brown noise caprock.

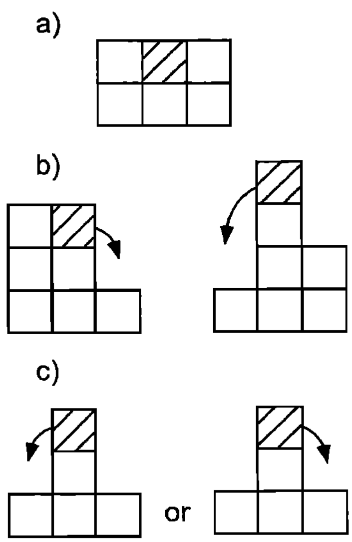

Figure 1. Illustration of the sediment deposition model. In each case a site is chosen randomly (the center of the three sites in each of the above pictures). The dotted block shows the unit of sediment being added to the surface. The arrows point toward the site upon which the unit of sediment will be deposited. (a) The chosen site has a lower elevation than either of its nearest neighbors, so the sediment is deposited at the chosen site. (b) One of the nearest neighboring sites has a lower elevation and the sediment is deposited at that lower site. (c) In the case of a tie for the lowest elevation between two or three sites, the site on which the sediment is deposited is chosen randomly between the sites of the same elevation.

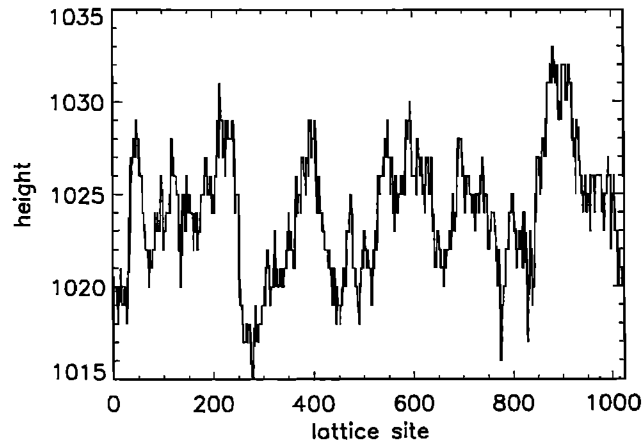

Figure 2. Surface constructed from the depositional model on a 1024 grid after the surface variance has reached saturation.

Model for Deposition in Fluvial Sedimentary Basins

We first consider a discrete model of channel avulsion and deposition. In each time step a site on a one-dimensional lattice is chosen at random. During that time step a unit of sediment is deposited at that site or one of its nearest neighbors depending on which site has the lowest elevation. This is the simplest model combining randomness and the tendency for sediment to be deposited in low-lying areas of the alluvial plain. This model is illustrated in Figure 1. The dotted block shows the unit of sediment being added to the surface. The arrows point toward the site upon which the unit of sediment will be deposited. In Figure 1a the chosen site has a lower elevation than either of its nearest neighbors, so the sediment is deposited at the chosen site. In Figure 1b one of the nearest neighboring sites has a lower elevation and the sediment is deposited at that lower site. In the case of a tie for the lowest elevation between two or three sites, the site on which the sediment is deposited is chosen randomly between the sites of the same elevation, as in Figure 1c. The local elevation is the total number of units of sediment that have been deposited at the site. This model of surface growth was first analyzed by *Family* [1986] with applications to the growth of atomic surface layers. He reported the results of computer simulations which showed that the model produces scale invariant variations of the surface in space and time. He found that the standard deviation σ of the surface follows the relation

$$\sigma(L,T) \propto L^{1/2}T^{1/4} \quad (1)$$

where L is a length scale and T is a timescale. Surfaces with scale invariant standard deviations $\sigma(L,T) \propto L^H T^K$ have a power law dependence of the power spectral density $S(k)$ on wavenumber k of the form $S(k) \propto k^{-2H-1}$ (i.e., $\propto k^{-2}$ for $H = 1/2$) and a power law de-

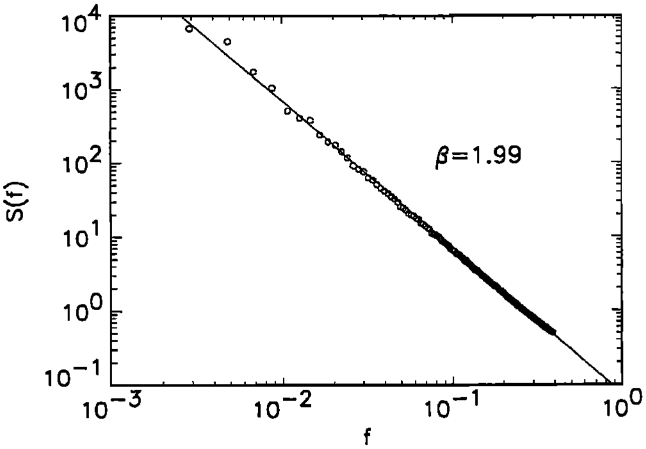

Figure 3. Average power spectrum of the surfaces constructed from 50 independent simulations on a 1024 grid as function of the wavenumber k. The model constructs a Brown noise surface.

pendence on frequency of the form $S(f) \propto f^{-2K-1}$ (i.e., $\propto f^{-3/2}$ for $K = 1/4$).

Figure 2 presents a surface produced by the model with a lattice size of 1024. We have run the simulation for some time to build up a rough surface. (The surface begins flat. Its variance saturates when the height equals the width of the lattice.) Figure 3 shows the average power spectrum of the surfaces produced by 50 independent simulations on a logarithmic scale. The power spectrum is proportional to k^{-2}, indicating that the surface is Brown noise. Other lattice sizes yield similar results. *Hooke and Rohrer* [1979] have mapped the topographic profiles of alluvial fans perpendicular to the flow direction. The Brown noise topography constructed by the model and presented in Figure 2 is strikingly similar to the alluvial fan profiles they present. Later in the paper we compare this model power spectrum to those of fluvial microtopographic transects obtained with laser altimetry.

In Figure 4 we plot the variations in surface elevation (subtracted from the mean height of the landscape) at the central site of our simulation after the surface variation has saturated. Figure 5 presents the average power spectrum of the difference from the mean height of the central site produced in 50 simulations. The power spectrum is proportional to $f^{-3/2}$.

We can also include the effects of erosion in our model. Although deposition generally occurs in topographic depressions, tending to smooth out the floodplain, erosion is less consistent. Erosion can downcut in a channel or, during a large flood, can lower alluvial ridges. We have modified our simulation to include the effects of erosion by choosing randomly at each time step whether to deposit or erode sediment during that time step. The probability of deposition must be greater than 0.5 in order to accumulate a sedimentary basin over time. We have studied the above model assuming that erosion occurs preferentially on channel floors, randomly on the landscape, or preferentially on alluvial ridges. In the simulation in which we assumed erosion to occur preferentially on the channel floors, we have included an erosion rule that takes away rather than deposits a unit of sediment at a randomly chosen site or one of its nearest neighbors, depending on which has the lowest elevation. We have also investigated rules that remove a unit of sediment from the chosen site always (to simulate random erosion on the floodplain) and a rule that removes sediment from the chosen site or one of its nearest neighbors, depending on which site is highest, to simulate the preferential erosion of alluvial ridges. The exponents of the power law power spectra we identified in the model without erosion is unchanged by including any of these erosion models.

In this model the probability that a particle is added to the site is proportional to two if both of a site's neighbors have a higher elevation, proportional to one if only one of the neighbors is higher, and zero if both neighbors

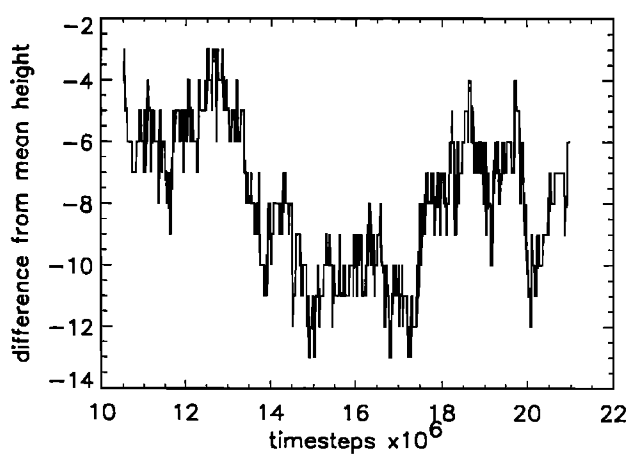

Figure 4. Difference from the mean height of the central site of the lattice after the surface variance has reached saturation.

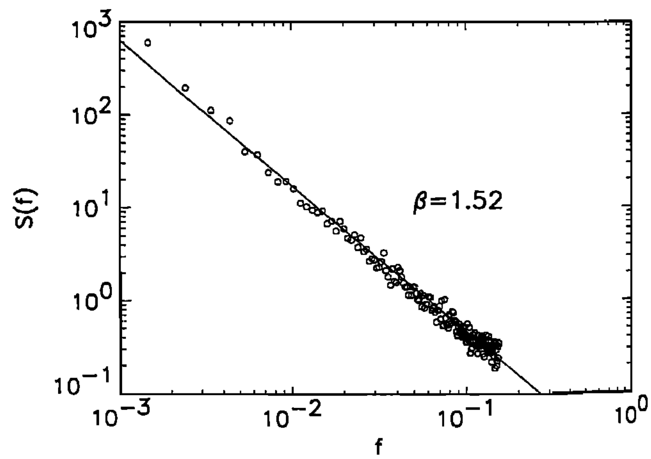

Figure 5. Average power spectrum of the difference from the mean height of the central site for 50 independent simulations as as a function of frequency in time steps^{-1}. The power spectrum is proportional to $f^{-3/2}$.

are lower. The model may be described mathematically with a stochastic difference equation of the form

$$h_{i,t+1} - h_{i,t} \propto H(h_{i+1,t}, h_{i,t}) + H(h_{i-1,t}, h_{i,t}) \quad (2)$$

where $h_{i,t+1} - h_{i,t}$ represents the most probable growth rate of the surface, and H is the Heavyside function defined by $H(x, x_o) = 1$ if $x > x_o$ or 0 if $x < x_o$. Averaging this equation over a time long compared to the time required to grow a single layer of unit height of sediment, the equation for the average surface growth rate is

$$\langle h_{i,t+1} - h_{i,t}\rangle \propto \langle h_{i+1,t} - h_{i,t}\rangle + \langle h_{i-1,t} - h_{i,t}\rangle \quad (3)$$

$$\propto \langle h_{i+1,t}\rangle - 2\langle h_{i,t}\rangle + \langle h_{i-1,t}\rangle \quad (4)$$

This is a discrete version of the diffusion equation. Directing sediment to lower elevations smooths out the surface and is equivalent to a diffusion process. As recognized by *Family* [1986], a continuous version of the discrete model is provided by a one-dimensional diffusion equation with a Gaussian white noise term:

$$\frac{\partial h(x,t)}{\partial t} = D\frac{\partial^2 h(x,t)}{\partial x^2} + \eta(x,t) \quad (5)$$

where $\eta(x,t)$ is the Gaussian white noise. This equation represents a model in which channels avulse randomly in time and space across the alluvial plain and sediment transport is governed by the diffusion equation. This equation and variants of it have been studied extensively in the physics literature (where it is known as the linear Langevin equation or the Edwards-Wilkinson equation) as a model for the growth of granular and atomic surfaces with random deposition of particles and subsequent diffusive relaxation [*Edwards and Wilkinson*, 1982; *Family*, 1986; *Barabasi and Stanley*, 1995]. The statistics of variations of the surface predicted by this equation were computed by *Edwards and Wilkinson* [1982]. The power spectra of surface variations in space and time computed analytically agree with the simulation results described above. In the appendix we include a somewhat different, more complete derivation based on power spectra rather than on the standard deviation that should be clearer to those not expert in stochastic processes. The inclusion of this rederivation of the Edwards-Wilkinson results also facilitates our derivation of the spectral exponents in the extension of this model to three dimensions (with a two-dimensional surface).

Most fluvial sedimentary environments, particularly meandering streams, do not have channels that are parallel. In the appendix we show that the scale invariant power spectra we have obtained is applicable to the structure of a two-dimensional surface when the assumption of parallel channels is relaxed and the channels, represented as straight lines, are allowed to obey any angular probability distribution.

Grain size variations mimic the topographic profile perpendicular to the channel direction with the coarsest material deposited at the channel banks and finer sediment deposited in topographic depressions. *Pizzuto* [1987] has sucessfully modeled the topography and grain size variations perpendicular to the channel direction with a diffusion equation. This coupling between grain size and topography suggests that porosity variations may exhibit the same power law power spectra as the topographic profile. A direct relationship between local profile elevation and grain size is also consistent with the observation of coarsening trends in aggrading channels as they are filled and approach the mean height of the profile of the floodplain [J. S. Bridge, unpublished manuscript, 1995]. Variations in local elevation in time have a power spectrum $S(f) \propto f^{-3/2}$ according to the model we present. If the mean elevation of the sedimentary basin relative to its base aggrades in a constant long-term average rate over time, time and depth are equivalent. In the next section we present evidence that vertical porosity variations are scale invariant with $\beta = 3/2$.

Observations of Vertical Porosity Variations in Sedimentary Basins

Porosity as a function of depth is routinely measured at equal intervals in formation well logs [*Hewett*, 1986]. As a specific example we have considered the porosity logs from 15 wells in the Gulf of Mexico. The wells are drilled in a deltaic sedimentary environment with a few large, nearly vertical faults [*Alexander*, 1995]. The simplest and most direct way to estimate the power spectrum of an evenly sampled series is to compute the modulus squared of the Fourier coefficients obtained from the Fast Fourier Transform (FFT). The power spectrum estimated in this way (with the FFT computed using the Numerical Recipes routine "realft" [*Press et al.*, 1992]) are plotted in Figures 6a and 6b as a function of the wavenumber k in m^{-1}. At spatial scales larger than 3 m the power spectra are well approximated by a power law. Below this scale the variability decreases sharply in most of the wells. This decrease in variability below the scale invariant trend may be the result of a transition from second-order heterogeneities (dominated by variations in porosity within the larger genetic units) to third order heterogeneities which result from the geometrical arrangements of individual depositional units. The transition from second- to third-order heterogeneities occurs on the scale of meters [*Allen and Allen*, 1990], consistent with the 3-m scale of the break observed in the power spectra. We estimated β from the slope of least squares linear fit to the logarithm (base 10) of the power spectra as a function of the logarithm of the wavenumber up to a scale of 3 m. The values of β obtained exhibit considerable variability from well to well. However, the average β equals 1.4 and is close to

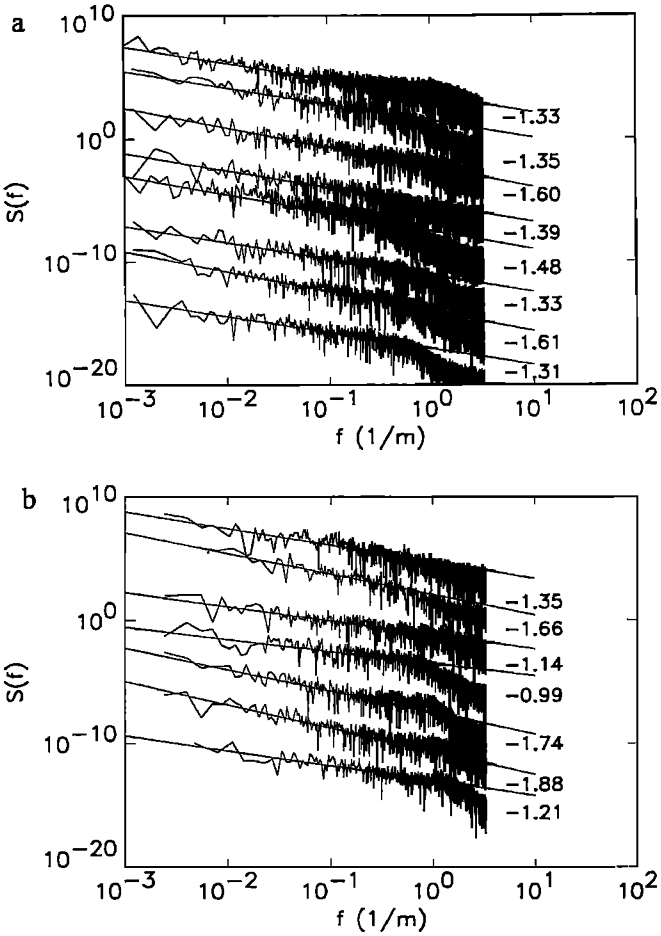

Figure 6. Power spectra of porosity as a function of wavenumber in units of m^{-1} in fifteen wells from the Gulf of Mexico. The spectra are offset so that they may be placed on the same graph.

the value of 1.5 predicted by the model. The standard deviation is 0.2.

A common feature of the vertical variation in grain size of deltaic sediments is a large-scale fining trend due to progradation of the delta along the flow direction. Our model does not attempt to model this trend, since we model only the profile perpendicular to the flow direction. While some of the large-scale variability of porosity may be attributed to progradation in the Gulf of Mexico, making the comparison of our model to the data problematic, any progradational trend cannot account for the scale invariance, since it acts on only the largest scales. This is supported by the work of *Holliger* [1996], who removed the large-scale trend in sonic logs with a low-order polynomial. The resulting spectral exponents were unchanged.

Two studies have reported ranges of βs from time series analyses of vertical density and porosity variations in well logs. *Holliger* [1996] has reported βs from 1.2 to 1.4, somewhat smaller, but roughly consistent with the values reported here. The values of β obtained by *Tubman and Crane* [1995] in their spectral studies of vertical well logs are considerably smaller than the values reported here (they report values between 1/2 and 1). However, they did not obtain their results directly from a spectral analysis. Instead, they determined a Hurst exponent from the rescaled-range analysis and inferred a value of β from that. One can see from their published spectra that least squares fits to their spectra imply a significantly larger value of β than those obtained by rescaled-range analysis. We prefer our methodology since there is evidence that the power spectrum is a more reliable and consistent method for quantifying β than the rescaled-range analysis. In a comparative study of the two methods, *Schepers et al.* [1992] concluded that power spectral analysis yielded the least biased results and the lowest variance in estimates of β, while the rescaled-range analysis gave biased results under many circumstances.

Brown Noise Topography in Fluvial Sedimentary Basins

Dunne et al. [1995] have performed power spectral analyses of fluvial microtopographic transects perpendicular to the fall line from two hillslopes obtained with laser altimetry from scales of 0.1 to 100 m. Their work provides us with a direct test of our model. They obtained power spectra with power law dependences. The exponents of the power spectra had an average of -1.6 with a standard deviation of 0.2, somewhat smaller than our model prediction of -2. Further modeling and observational work will be necessary to determine the reason for this discrepancy.

Barton and Scholz [1995] have presented the spatial distribution of drilled wells and wells showing hydrocarbons in the Denver and Powder River basins. These basins evolved from deposition in a meandering alluvial environment [*Berg*, 1968]. Using the box counting technique Barton and Scholz found that the fractal dimensions for the drilled wells in the two basins were 1.80 and 1.86 and that the fractal dimensions of the showing wells were 1.43 and 1.49, respectively. The accumulation of petroleum will be determined by the spatial distribution of source and trap rocks. After petroleum is generated and expelled from source rocks, it will move from sites of high potential energy to sites of low potential energy. Hydrocarbons are often found adjacent to the crests of low-porosity caprock that have obstructed its upward migration [*Allen and Allen*, 1990]. The caprock will mimic the floodplain relief at the time of its deposition. This is consistent with the observation that hydrocarbons are often found in geometries which mimic the topography of the alluvial plain at the time of deposition in a variety of fluvial depositional environments such as meandering [*Curry and Curry*, 1972], deltaic [*Coleman and Prior*, 1982], and submarine fans [*Garcia*, 1981; *Wilde et al.*, 1978]. A simple model for the horizontal spatial distribution of hydrocarbons in a reservoir is one in which hydrocarbons are assumed to be accumulated

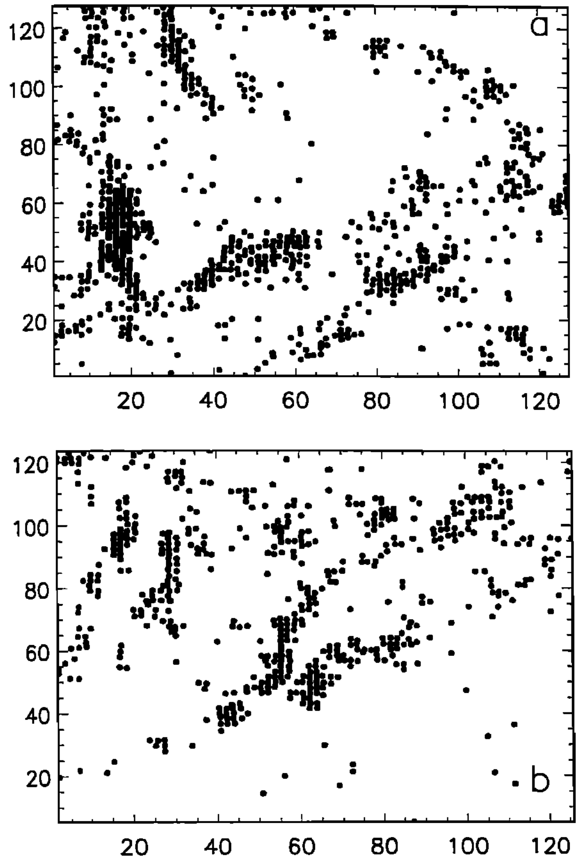

Figure 7. Wells producing hydrocarbons in the (*a*) Powder River and (*b*) Denver basins. Distance units are scaled such that the basin is 128 x 128.

in all of the crests of the caprock above a certain elevation. This model ignores, however, the possible steering effects of migration pathways.

The spatial distribution of showing wells in the Powder River and Denver basins are given in Figures 7a and 7b. We have set the width of the basin to be 128 so as to facilitate comparisons with a synthetic reservoir constructed on a 128 x 128 grid. We analyzed the data with the pair correlation function which we believe to be a better estimator of correlations for point processes than box counting. The exponent of the number of blocks N as a function of box size r, which defines the fractal dimension, is not constant over the spatial range of the data analyzed by *Barton and Scholz* [1995] but shows a gradual variation from 2 (at large scales) to 1 (at small scales). Our plots exhibit a more consistent trend over the spatial range of the data.

The two-dimensional pair correlation function $C(r)$ is defined as the number of pairs of wells whose separation is between r and $r + \Delta r$, per unit area [*Vicsek*, 1992]. The pairs are binned in logarithmically spaced intervals Δr. For a data set with scale invariant clustering, $C(r) \propto r^{-\alpha}$ where α is related to the fractal dimension through $D = 2 - \alpha$ in two dimensions [*Vicsek*, 1992]. The pair correlation function is commonly employed in the analysis of diffusion-limited-aggregation. However, studies incorporating it in the Earth sciences are rare. *Kagan and Knopoff* [1980] have applied it to the spatial clustering of earthquakes.

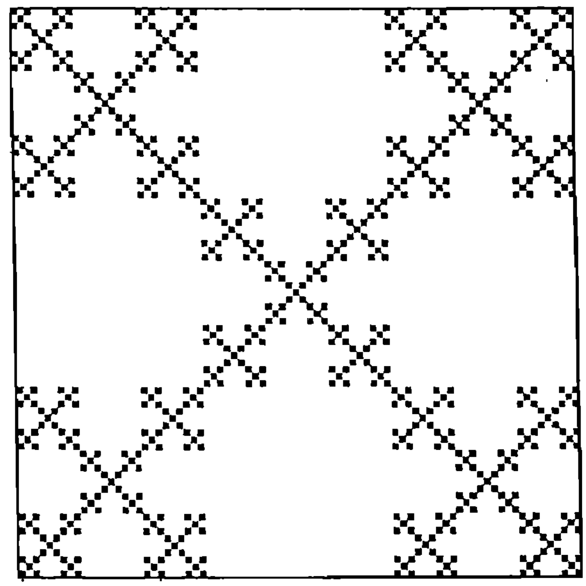

Figure 8. Order 4 construction of the Koch snowflake.

As an example of the pair correlation function on a traditional fractal, we have calculated the fractal dimension of the Koch snowflake of Figure 8. The pair correlation function of the Koch snowflake is presented in Figure 9. The pair correlation function of a random, uncorrelated, Poisson distribution would be exponential. The straight line form of the pair correlation function of the Koch snowflake on a log-log plot indicates scale invariant clustering and long-range correlations. The fractal dimension inferred from the slope of this data is D = 1.42, close to the exact value of 1.46. Figure 10 shows the pair correlation function of the Denver and Powder River basin wells on a log-log plot. The least squares fit to the correlation function yields an expo-

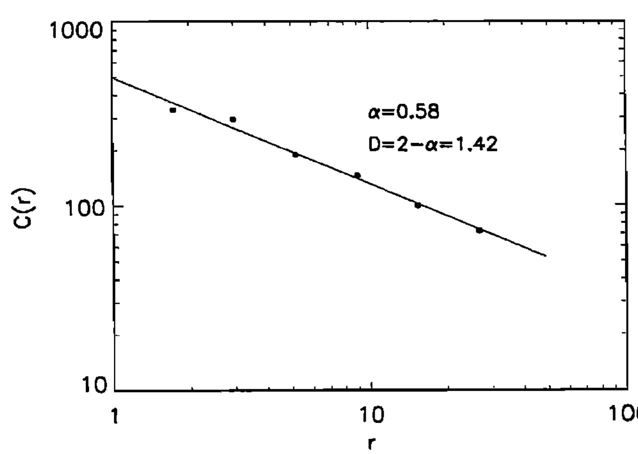

Figure 9. Pair correlation function of the Koch snowflake of Figure 8.

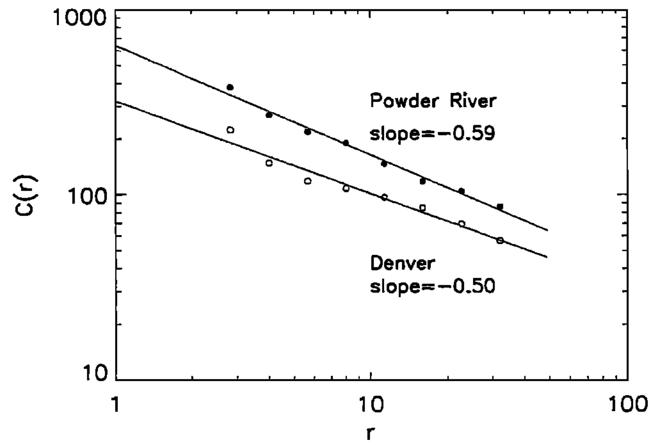

Figure 10. Pair correlation function of the (top) Powder River and (bottom) Denver basins as a function of the pair separation.

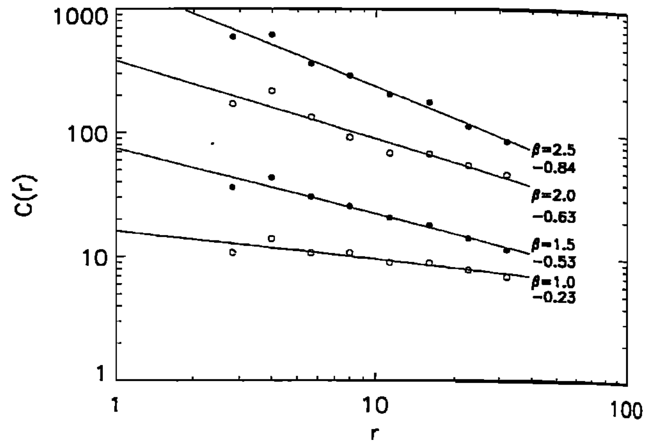

Figure 12. Pair correlation functions for synthetic reservoirs like the one in Figure 11 with different β values. The plots are offset so that they may be placed on the same graph.

nent of $\alpha = -0.59$ for Powder River and $\alpha = -0.50$ for the Denver basin, implying $D = 1.41$ and $D = 1.5$, respectively. The results obtained by the pair correlation method are in close agreement with the results obtained by *Barton and Scholz* [1995] using box counting.

To show that these correlation functions are consistent with a caprock with Brownian topography, we have constructed synthetic reservoirs where hydrocarbons are showing in regions where the caprock elevation in larger than a threshold value. In order to do this we synthesized a two-dimensional noise on a 128 x 128 lattice with the Fourier-filtering technique described by *Turcotte* [1992]. The threshold value for showing hydrocarbons was chosen such that the resulting synthetic reservoir had the same percentage of showing wells as the Denver and Powder River basins (about 5%). Figure 11 shows a synthetic reservoir produced with $\beta = 2.0$ (Brown noise). The synthetic reservoir shows a degree of clustering similar to the Denver and Powder River basins. In Figure 12 we have plotted the pair correlation functions for the showing wells in synthetic reservoirs constructed with $\beta = 2.5$, 2.0, 1.5, and 1.0. The pair correlation functions show a gradual decrease with decreasing β. The synthetic reservoirs whose scaling exponents α most closely match those of the Denver and Powder River basins are $\beta = 2.0$ and $\beta = 1.5$. Although we cannot precisely determine the scaling exponent of the porosity variations with this method, we conclude that β is close to 2, consistent with our model.

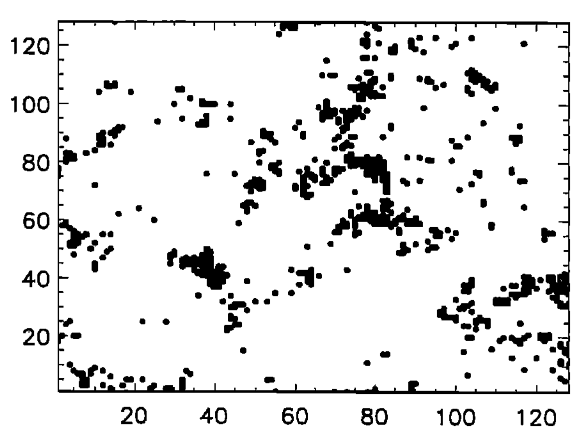

Figure 11. Synthetic reservoir constructed with a caprock of Brown noise constructed on a 128 x 128 grid where all the sites with porosity greater than a fixed level are showing.

Besides the pair correlation function, two other fractal relations allow us to infer Brown noise paleotopography from horizonal variations in sedimentary basins. *Agterberg* [1982] has computed the fractal dimension of the perimeter of sand isopach contours from the Lloydminster oil field to be 1.3, close to the value of 1.25 measured for coastlines and topographic contours [*Turcotte*, 1992]. *Barton and Scholz* [1995] have presented plots which show that the cumulative number of oil fields has a power law dependence on the volume of the fields with exponent close to -1: $N(>V) \propto V^{-1}$. *Kondev and Henley* [1995] have related the length distribution of contour lengths of Gaussian surfaces to the roughness or Hurst exponent. J. D. Pelletier [Kardar-Parisi-Zhang model for the growth of the convective boundary layer and cumulus cloud fields, submitted to *Physical Review Letters*, 1996] has shown that their results imply that the cumulative frequency-area distribution of areas enclosed by contours of a Brown noise surface is $N(>A) \propto A^{-3/4}$. Since oil fields have a much larger horizontal extent than vertical extent, it is reasonable to assume that area and volume are proportional. Our model of hydrocarbon shows in regions with caprock topography above a threshold elevation then predicts $N(>V) \propto V^{-3/4}$ in reasonable agreement with the cumulative frequency-size distributions of *Barton and Scholz* [1995].

Conclusions

We have shown that a simple model of an alluvial plain evolving with channel avulsion, deposition, and erosion predicts a scale invariant topographic profile in space and time. Observed power spectra of fluvial microtopography is roughly consistent with Brown noise. We inferred Brown noise paleotopography by comparing the pair correlation function of showing wells in the Denver and Powder River basins with a synthetic oil field based on a caprock with Brown noise topography. We also presented evidence supporting our hypothesis that variations in porosity are coupled to the topographic profile by computing the power spectrum of vertical porosity well logs from the Gulf of Mexico.

Appendix: Calculation of the Scaling Exponents of the Continuous Model

In order to calculate the power spectra of the surface variations resulting from the linear Langevin equation with a one-dimensional surface, equation (5), we Fourier expand the surface, $h(x,t)$ in space and time in terms of its Fourier transform $a(k,\omega)$:

$$h(x,t) = \int_{-\infty}^{\infty} dk \int_{-\infty}^{\infty} d\omega\ a(k,\omega) e^{ikx} e^{i\omega t} \tag{A1}$$

$$a(k,\omega) = \frac{1}{(2\pi)^2} \int_{-\infty}^{\infty} dx \int_{-\infty}^{\infty} dt\ h(x,t) e^{-ikx} e^{-i\omega t} \tag{A2}$$

The power spectrum of $h(x,t)$ in space at a point in time is the power spectrum $S(k,\omega)$ inverse Fourier-transformed back to a function of time and evaluated at $t=0$. The power spectrum $S(k,\omega)$ is related to the Fourier coefficients as [*Toda et al.*, 1992]

$$\langle a(k,\omega) a^*(k',\omega)\rangle = S(k,\omega)\delta(k-k') \tag{A3}$$

where the asterisk denotes the complex conjugate and the brackets represent an average over all possible realizations of the process (an "ensemble average"). Integrating over k we get

$$S(k,\omega) = \langle a(k,\omega) a^*(k,\omega)\rangle \tag{A4}$$

The Fourier transform of the linear Langevin equation is

$$i\omega a(k,\omega) - Dk^2 a(k,\omega) = \eta(k,\omega) \tag{A5}$$

Solving this equation for $a(k,\omega)$, multiplying by its complex conjugate, and taking an ensemble average of both sides we obtain

$$< a(k,\omega)a^*(k,\omega) > = \frac{< \eta(k,\omega)\eta^*(k,\omega) >}{\omega^2 + D^2k^4} \tag{A6}$$

Since the noise term $\eta(k,\omega)$ is white noise, its correlation $\langle \eta(k,\omega)\eta^*(k,\omega)\rangle$ is constant as a function of k and ω. Equations (A4) and (A6) then give

$$S(k,\omega) \propto \frac{1}{D^2k^4 + \omega^2} \tag{A7}$$

Fourier-transforming back to time,

$$S(k,t) \propto \int_{-\infty}^{\infty} d\omega \frac{e^{i\omega t}}{D^2k^4+\omega^2} \tag{A8}$$

$$\propto \frac{e^{-k^2Dt}}{k^2} \tag{A9}$$

which is $\propto k^{-2}$ when evaluated at $t=0$.

To obtain the power spectrum of variations in the surface as a function of time at a point in space, we Fourier-transform (A7) to space and evaluate the resulting function at $x=0$:

$$S(x,\omega) \propto \int_{-\infty}^{\infty} dk \frac{e^{ikx}}{D^2k^4+\omega^2} \tag{A10}$$

$$\propto \frac{1}{\omega^{\frac{3}{2}}}(\cos(ax') + \sin(ax'))(\cosh(ax') - \sinh(ax')) \tag{A11}$$

where

$$a = \sqrt{\frac{\omega}{2D}} \tag{A12}$$

which is $\propto \omega^{-3/2}$ when evaluated at $x=0$.

We next consider solving the three-dimensional linear Langevin equation with randomly directed line noise (the amplitude of the noise is Gaussian, its position and orientation are uniformly random). The lines represent channels in which sediment is eroded or deposited on the alluvial plain. An analysis of a similar system driven by line noise was performed by *Nelson and Radzihovsky* [1992]. We follow their approach. We will calculate the power spectrum in three dimensions, $S(k,\omega)$, where $k=\sqrt{k_x^2+k_y^2}$. The subset of lines directed along the y direction is

$$\eta_l(x,y) = \sum_j \eta_j \delta_{lx}\delta(x-x_j) \tag{A13}$$

where η_j is the amplitude of the jth line with x coordinate x_j, the index l (and later m) stands for the x or y direction, and the δ variables are the Dirac delta functions. If the x_j variables are random and we generalize the above to allow the set of parallel lines to run in any direction with normal vector $\hat{n}$, the ensemble average of line noise with normal vector $\hat{n}$ is given by

$$\langle \eta_l(\vec{k})\eta_m^*(\vec{k})\rangle_{\hat{n}} \propto \delta(\hat{n}\cdot\vec{k}) \tag{A14}$$

Averaging over all possible directions for $\hat{n}$, this expression becomes [*Nelson and Radzihovsky*, 1992]

$$\langle \eta_l(\vec{k})\eta_m^*(\vec{k})\rangle \propto \frac{1}{k}\frac{k_l k_m}{k^2} \tag{A15}$$

where $k=\sqrt{k_x^2+k_y^2}$. The ensemble average of the noise is no longer constant as it was for point noise; it is $\propto k^{-1}$. As a result, the three-dimensional power spectrum will be

$$S(k,t) \propto \int_{-\infty}^{\infty} d\omega \frac{1}{k} \frac{e^{i\omega t}}{D^2k^4+\omega^2} \quad \text{(A16)}$$

$$\propto k^{-3} \quad \text{(A17)}$$

when evaluated at $t = 0$. The two-dimensional power spectrum is related to β through $S(k) \propto k^{-\beta-1}$ [*Turcotte*, 1992]. The extra factor of k^{-1} in this expression comes from the factor of k in the radial differential $k\ dk$ in two spatial dimensions. Thus $\beta = 2$ for this model, yielding the same one-dimensional power spectrum as with the two-dimensional linear Langevin equation with point noise. In the integral $S(0,\omega) \propto \omega^{-3/2}$ since the radial differential cancels out the $1/k$ yielding the same integral as in (A10).

If the distribution of line noise has an angular dependence, this does not change the form of the power spectrum. The only change in the above analysis will be to modify (A15) by a constant factor.

Acknowledgments. We wish to thank Alberto Malinverno and an anonymous reviewer for critical reviews of the manuscript. We thank Bruce Malamud, Arthur Bloom, Teresa Jordan, Brooke Eiche, Larry Cathles, and Fereydoon Family for helpful conversations. We are further indebted to Brooke Eiche for providing us with the well log data.

References

Agterberg, F.P., Recent developments in geomathematics, *Geoprocessing, 2*, 1-32, 1982.

Alexander, L.L., Geologic evolution and stratigraphic controls on fluid flow of the Eugene Island Block 330 Mini Basin, offshore Louisiana, Ph.D. dissertation, Cornell Univ., Ithaca, N. Y., 1995.

Allen, P.A., and J.R. Allen, *Basin Analysis: Principles and Applications*, Blackwell Sci., Cambridge, Mass., 1990.

Barabasi, A.-L., and H.E. Stanley, *Fractal Concepts in Surface Growth*, chap. 5, Cambridge Univ. Press, New York, 1995.

Barton, C.C., and C.H. Scholz, The fractal size and spatial distribution of hydrocarbon accumulations: implications for resource assessment and exploration strategy, in edited by C.C. Barton and P.R. LaPointe, *Fractals in Petroleum Geology and Earth Sciences*, pp. 13-34, Plenum, New York, 1995.

Berg, R.R., Point bar origin of Fall River sandstone reservoirs, northeast Wyoming, *Am. Assoc. Pet. Geol. Bull., 52*, 2116-2122, 1968.

Bridge, J.S., and M.R. Leeder, A simulation model of alluvial stratigraphy, *Sedimentology, 26*, 617-644, 1979.

Coleman, J.M., and D.B. Prior, Deltaic environments of deposition, in *Sandstone Depositional Environments*, edited by P.A. Scholle and D. Spearing, *AAPG Mem., 31*, 139-178, 1982.

Culling, W.E.H., Theory of erosion of soil-covered slopes, *J. Geol., 73*, 230-254, 1965.

Curry, W.H., and W.H. Curry III, South Glennock oil field, Wyoming: A pre-discovery thinking and post-discovery description, in *Stratigraphic Oil and Gas Fields*, edited by R.E. King, *Mem. Am. Assoc. Pet. Geol., 15*, 415-427, 1972.

Dunne, T., K.X. Whipple, and B.F. Aubry, Microtopography of hillslopes and initiation of channels by Horton overland flow, in *Natural and Anthropogenic Influences in Fluvial Geomorphology: The Wolman Volume, Geophys. Monogr. Ser.*, vol. 89, edited by J.E. Costa et al., pp. 27-44, AGU, Washington, D. C., 1995.

Edwards, S.F., and D.R. Wilkinson, The surface statistics of a granular aggregate, *Proc. R. Soc. London A, 381*, 17-31, 1982.

Family, F., Scaling of rough surfaces: Effects of surface diffusion, *J. Phys. A Math. Gen., 19*, L441-L446, 1986.

Fox, C.G., and D.E. Hayes, Quantitative methods for analyzing the roughness of the seafloor, *Rev. Geophys., 23*, 1-48, 1985.

Garcia, R., Depositional systems and their relation to gas accumulation in Sacremento Valley, California, *AAPG Bull., 65*, 653-674, 1981.

Hanks, T.C., R.C. Buckman, K.R. Lajoie, and R.E. Wallace, Modification of wave cut and faulting-controlled landforms, *J. Geophys. Res., 89*, 5771-5790, 1984.

Hanks, T.C., and R.E. Wallace, Morphological analysis of the Lake Lahontan shoreline and beachfront fault scarps, Pushing County, Nevada, *Bull. Seismol. Soc. Am., 75*, 835-846, 1985.

Hewett, T.A., Fractal distribution of reservoir heterogeneity and their influence of fluid transport, *SPE Prof. Pap.* 15386, Soc. of Pet. Eng., Richardson, Tex., 1986.

Hirst, J.P.P., C.R. Blackstock, and S. Tyson, Stochastic modeling of fluvial sandstone bodies, in *The Geological Modeling of Hydrocarbon Reservoirs*, edited by S. Flint and I.D. Bryant, *Spec. Pub. 15*, pp. 237-252, Int. Assoc. of Sedimentol., 1993.

Holliger, K., Upper-crustal seismic velocity heterogeneity as derived from a variety of P-wave sonic logs, *Geophys. J. Int., 125*, 813-829, 1996.

Hooke, R.L., and W.L. Rohrer, Geometry of alluvial fans: Effects of discharge and sediment size, *Earth Surf. Processes, 4*, 147-166, 1979.

Kagan, Y.Y., and L. Knopoff, Spatial distribution of earthquakes: The two-point correlation function, *Geophys. J. R. Astron. Soc., 62*, 303-320, 1980.

Kenyon, P.M., and D.L. Turcotte, Morphology of a delta prograding by bulk sediment transport, *Geol. Soc. Am. Bull., 96*, 1457-1465, 1985.

Kondev, J., and C.L. Henley, Geometrical exponents of contour loops on random Gaussian surfaces, *Phys. Rev. Lett., 74*, 4580-4584, 1995.

Leeder, M.R., A quantitative stratigraphic model for alluvium, with special reference to channel deposit density and interconnectedness, in *Fluvial Sedimentology*, edited by A.D. Miall, *Mem. Can. Soc. Pet. Geol., 5*, 587-596, 1978.

Mackey, S.D., and J.S. Bridge, Three-dimensional model of alluvial stratigraphy: Theory and application, *J. Sediment. Res. Sect. B, 65*, 7-31, 1995.

Molz, F.J., and G.K. Boman, A fractal-based stochastic interpolation scheme in subsurface hydrology, *Water Resour. Res., 29*, 3769-3774, 1993.

Nash, D.B., Morphologic dating of degraded normal fault scarps, *J. Geol., 88*, 353-360, 1980a.

Nash, D., Forms of bluffs degraded for different lengths of time in Emmet County, Michigan, USA, *Earth Surf. Processes, 5*, 331-345, 1980b.

Nelson, D.R., and L. Radzihovsky, Grain-boundary instabilities and buckling in partially polymerized membranes, *Phys. Rev. A, 46*, 7474-7479, 1992.

Pilkington, M., and J.P. Todoeschuck, Stochastic inversion for scaling geology, *Geophys. J. Int., 102*, 205-217, 1990.

Pizzuto, J.E., Sediment diffusion during overbank flows, *Sedimentology, 34*, 301-317, 1987.

Press, W.H., S.A. Teukolsky, W.T. Vetterling, and B.P. Flannery, *Numerical Recipes in C: The Art of Scientific Computing*, 2nd ed., Cambridge Univ. Press, New York, 1992.

Schepers, H.E., J.H.G.M. van Beek, and J.B. Bassingthwaighte, Four methods to estimate the fractal dimension from self-affine signals, *IEEE Eng. in Med. and Bio., 11*, 57-64, 1992.

Sornette, D., and Y.-C. Zhang, Non-linear Langevin model of geomorphic erosion processes, *Geophys. J. Int., 113*, 382-386, 1993.

Toda, M., R. Kubo, and N. Saito, *Statistical Physics II: Nonequilibrium Statistical Mechanics*, Springer-Verlag, New York, 1992.

Todoeschuck, J.P., and O.G. Jensen, Scaling geology and seismic deconvolution, *Pure Appl. Geophys., 131*, 273-287, 1989.

Todoeschuck, J.P., O.G. Jensen, and S. Labonte, Gaussian scaling noise model of seismic reflection sequences: Evidence from well logs, *Geophysics, 55*, 480-484, 1990.

Tubman, K.M., and S.D. Crane, Vertical versus horizontal well log variability and application to fractal reservoir modeling, in *Fractals in Petroleum Geology and Earth Sciences*, edited by C.C. Barton and P.R. LaPointe, pp. 279-294, Plenum, New York, 1995.

Turcotte, D.L., A fractal interpretation of topography and geoid spectra on the Earth, Moon, Venus, and Mars, *J. Geophys. Res. 92*, 597-601, 1987.

Turcotte, D.L., *Fractals and Chaos in Geology and Geophysics*, Cambridge Univ. Press, New York, 1992.

Vicsek, T., *Fractal Growth Phenomena*, World Sci., River Edge, N. J., 1992.

Walden, A.T., and J.W.J. Hosken, An investigation of the spectral properties of primary reflection coefficients, *Geophys. Prospect., 33*, 400-435, 1985.

Wallace, R.E., Profiles and ages of young fault scarps, north-central Nevada, *Geol. Soc. Am. Bull., 88*, 1267-1281, 1977.

Wilde, P., W.R. Normark, and T.E. Chase, Channel sands and petroleum potential of Monterey deep-sea fan, California, *AAPG Bull., 62*, 967-983, 1978.

J. D. Pelletier and D. L. Turcotte, Department of Geological Sciences, Snee Hall, Cornell University, Ithaca, NY 14853. (e-mail: pelletie@geology.cornell.edu; petricola@geology.cornell.edu)

(Received September 22, 1995; revised July 15, 1996; accepted September 18, 1996.)